2023 62nd IEEE Conference on Decision and Control (CDC)
December 13-15, 2023. Marina Bay Sands, Singapore

Formation Tracking Control of Heterogeneous Underactuated Planar Agents with Stable Internal Dynamics

Quoc Van Tran

Abstract— **Distributed formation tracking control of a system of heterogeneous underactuated agents on a 2-D plane is proposed based on the leader-follower approach and using the inter-agent displacements. A typical example of such an agent is an underactuated surface vessel whose planar surge-sway-yaw motion is considered, while only two independent controls are available, thus underactuated. Formation tracking control law is developed to steer certain offset points on the longitudinal axes of the agents, called *hand points*, to the target formation asymptotically and exponentially fast in the presence of bounded disturbances. A distinct feature of such an underactuated planar vehicle is that its lateral motion representing the non-actuated degree of freedom is unrestricted and can be unstable. Thus, a sufficient condition on the the leader's velocity and the hand points' locations for the stability of the lateral motion of the agents is provided. Simulation results of formation tracking control of underactuated surface vessels support the theoretical analysis.**

I. Introduction

Distributed coordination of a fleet of multiple autonomous agents has attracted considerable research attention in the last two decades [1]–[5]. In such a multi-agent system, the individuals sense nearby agents, communicate with each other, and perform certain actions based on the local information to achieve a group task.

Common planar agents, such as surface vessels, operating on a two-dimensional horizontal plane possess three degrees-of-freedom (surge, sway, and yaw) when neglecting the heave, roll, and pitch dynamics [6]. If there exist only two independent control forces, the system is said to be *underactuated* since the dimension of the configuration space (3 DOFs) is larger than the number of the control inputs. Note importantly how an underactuated agent is essentially different from a nonholonomic agent (e.g., wheeled vehicles [7]). First, due to the lack of a lateral motion constraint, the velocity of an underactuated vehicle need not be tangent to the motion path, unlike that of a unicycle ground vehicle. For unicycle robots, since their lateral motion is constrained, a typical tracking control approach is aligning their headings to a nominal control flow which is designed at the kinematic level (i.e., as reference velocity) [8]. In contrast, for the class of underactuated agents under study, the sway velocity associated with the uncontrolled lateral motion is free-floating and thus it can increase infinitely. As a result, one cannot straightforwardly apply kinematic control laws for nonholonomic agents [8] to the tracking control of underactuated agents. Therefore, one must design a tracking controller as forces/torques based on the nonlinear dynamics of underactuated agents while ensuring the ultimate boundedness of their lateral motion [9]. Third, the proposed tracking controller needs to be robust to model uncertainties and disturbances present in the environment. For example, underactuated surface vessels working in a marine environment are subject to ocean wind and water waves.

The coordination control of a group of planar agents has been investigated extensively [8], [10]–[13]. Nevertheless, few formation tracking control protocols have been proposed for planar agents with a *free-floating* lateral motion, e.g., surface vehicles, based largely on the leader-follower approach [9], [14]–[17] and virtual structure methods [9]. In virtual structure methods, each agent keeps up with a virtual leader which represents the agent's desired location in the target formation. As a result, the formation tracking task is decomposed into the tracking control of each agent. The simplest leader-follower method is for each follower to maintain a prespecified offset to a common leader [14], [15], resulting in a star network with the leader at the center. The leader is assumed to be able to follow a desired (formation) trajectory. The works [9], [16] proposed tracking control protocols for underactuated surface vessels with an acyclic (no directed loops) directed graph and one leader being the root node. In [9], sliding mode tracking controllers were presented based on either the distances or the relative positions between neighboring agents. The authors in [16] explored a control law for formation tracking of underactuated surface vessels, which requires a persistently exciting yaw rate of the leader. [17] addressed scaling control for formation with acyclic directed graphs based on inter-agent bearings. Formation tracking controllers were presented in our recent work [13] for underactuated surface vessels with a bearing rigid graph and based on the inter-agent bearings.

This work addresses formation tracking control for a system of heterogeneous underactuated agents in 2-D in the presence of bounded disturbances using inter-agent displacements. As the first contribution of this work, a general nonlinear dynamics with two independent control forces is presented for a type of planar agents, illustrated via the dynamic model of underactuated surface vessels. Then, a formation tracking control scheme is proposed for the system with an interaction graph containing a spanning tree and a leader being the root node, whose objective is steering certain points on the longitudinal axes, referred to as hand points,

Q. V. Tran is with the Department of Mechatronics, School of Mechanical Engineering, Hanoi University of Science and Technology (HUST), Hanoi, Vietnam. (e-mail: quoc.tranvan@hust.edu.vn)

This research is funded by Hanoi University of Science and Technology (HUST) under project number T2022-TT-004.

of the agents to the target formation. Second, exponential convergence to the target formation of the system is shown and a sufficient condition for uniform ultimate boundedness of the non-actuated lateral motion is provided. On the contrary, the boundedness of the lateral motion is often assumed in related works [14]–[17]. As a development of [13], the control approach developed for surface vessels is generalized for a class of underactuated planar agents interacting over a directed graph.

The remainder paper is structured as follows. Section II gives preliminaries and the problem statement. The proposed tracking control protocol is proposed and the stability analysis is established in Section III. Simulation results are provided in Section IV. Finally, Section V gives concluding remarks on this work.

II. Preliminaries and Problem Statement

Notation: We use $\mathbb{R}$ and $\mathbb{R}^d$ to denote the sets of real numbers and real d-dimensional vectors, respectively. The cross product is $\times$. Vectors expressed in a local coordinate frame $\{\mathcal{B}_i\}$ and the inertial frame $\{\mathcal{I}\}$ are denoted as $\boldsymbol{y}^i$ with superscript and $\boldsymbol{y}$, respectively. Free vectors with no need for a coordinate system to express them are denoted as $\vec{\boldsymbol{a}}$. For $\boldsymbol{x} \in \mathbb{R}^n$, $\mathrm{sign}(\boldsymbol{x})$ and $|\boldsymbol{x}| \in \mathbb{R}^n$ are the element-wise signum and absolute vectors, respectively. The $n \times n$ identity matrix is $\boldsymbol{I}_n$ and $\mathbf{1}_n = [1, \ldots, 1]^\top \in \mathbb{R}^n$. The stack vector $\mathrm{col}(\boldsymbol{z}_1, \ldots, \boldsymbol{z}_n) = [\boldsymbol{z}_1^\top, \ldots, \boldsymbol{z}_n^\top]^\top$ is obtained by placing $\boldsymbol{z}_1, \ldots, \boldsymbol{z}_n$ vertically one on top of each other. The notations $||\cdot||_1$ and $||\cdot||_\infty$ denote the 1-norm and infinity norm, respectively.

A. Mathematical structure of multi-agent networks

A multi-agent network is modeled as a directed graph (digraph) $\mathcal{G} = (\mathcal{V}, \mathcal{E})$ containing a set $\mathcal{V} = \{1, \ldots, n\}$ of n nodes and a set of edges $\mathcal{E} \subseteq \mathcal{V} \times \mathcal{V}$. Each edge $(i,j), i,j \in \mathcal{V}$, is directed with the source node i and sink node j. An undirected edge (i,j) is considered as containing two directed edges (i,j) and (j,i). The neighbor collection of i is given by $\mathcal{N}_i = \{j \in \mathcal{V} : (i,j) \in \mathcal{E}\}$. Fix an orientation of the m edges $\{e_1, \ldots, e_m\}$ between the nodes in $\mathcal{V}$ ($m = |\mathcal{E}|$), the incidence matrix is $\boldsymbol{H} = [h_{ik}] \in \mathbb{R}^{n \times m}$ as $h_{ik} = 1$ if $e_k = (j,i)$, $h_{ik} = -1$ if $e_k = (i,j)$, and $h_{ik} = 0$ otherwise. The Laplacian matrix $\mathcal{L} = [l_{ij}]$ associated with $\mathcal{G}$ is defined as $l_{ij} = -1$ for $(i,j) \in \mathcal{E}$, $i \neq j$, $l_{ii} = -\sum_{j \in \mathcal{N}_i} l_{ij}$, $\forall i = 1, \ldots, n$, and $l_{ij} = 0$ otherwise. If the undirected version of $\mathcal{G}$ is connected, we have $\mathrm{rank}(\boldsymbol{H}(\mathcal{G})) = n-1$ and $\boldsymbol{H}(\mathcal{G})^\top \mathbf{1}_n = \mathbf{0}$ [18].

B. The dynamics of underactuated planar agents

A group of n underactuated planar agents consists of one leader and $n-1$ *followers* having a sensing digraph $\mathcal{G} = (\mathcal{V}, \mathcal{E})$. Provide each agent i with a local coordinate system, $\{\mathcal{B}_i(x_{bi}, y_{bi})\}$, whose origin is at its center of mass or pivot point (see Fig. 1), with regard to which it observes the outside world. The position vector and yaw angle of agent i with regard to the inertial coordinates are $\boldsymbol{p}_i = [x_i, y_i]^\top \in \mathbb{R}^2$ and $\psi_i \in \mathbb{R}$, respectively. The velocity of agent i in $\{\mathcal{B}_i\}$ and its yaw rate are denoted as $\boldsymbol{v}_i^i = [u_i, \nu_i]^\top \in \mathbb{R}^2$ and $r_i \in \mathbb{R}$, respectively. The kinematics and a general nonlinear dynamics in $\{\mathcal{B}_i\}$ of each agent i is

$$\dot{\boldsymbol{p}}_i = \begin{bmatrix} \cos(\psi_i) & -\sin(\psi_i) \\ \sin(\psi_i) & \cos(\psi_i) \end{bmatrix} \begin{bmatrix} u_i \\ \nu_i \end{bmatrix} := \boldsymbol{R}_i(\psi_i)\boldsymbol{v}_i^i, \quad (1)$$

$$\dot{\psi}_i = r_i, \quad (2)$$

$$\begin{cases} \dot{u}_i = f_{ui}(u_i, \nu_i, r_i) + \delta_{ui}(t) + b_{ui}F_i \\ \dot{\nu}_i = f_{\nu i}(u_i, \nu_i, r_i) + \delta_{\nu i}(t) + b_{\nu i}T_i \\ \dot{r}_i = f_{ri}(u_i, \nu_i, r_i) + \delta_{ri}(t) + b_{ri}T_i. \end{cases} \quad (3)$$

Here, $\boldsymbol{R}_i(\psi_i) \in SO(2)$ denotes the rotation from the system $\{\mathcal{B}_i\}$ to $\{\mathcal{I}\}$, $f_{ki}(\cdot), k \in \{u, \nu, r\}$, are locally Lipschitz continuous functions, $b_{()}$.'s are certain constants, $\delta_{(\cdot)}$'s are bounded disturbances, the scalars F_i and T_i are two independent control inputs (e.g., longitudinal force and yaw moment). Note how the lateral and rotational motions (the second and third rows in (3)) cannot be controlled independently by only one control, i.e., T_i. Furthermore, the general nonlinear dynamics (3) can represent distinct dynamical models of planar underactuated agents, as we now illustrate using the dynamic model of surface vessel models.

Example 1: For illustration, consider the dynamics of underactuated surface vessels i given as follows [6]

$$\begin{bmatrix} m_{11} & 0 & 0 \\ 0 & m_{22} & m_{23} \\ 0 & m_{23} & m_{33} \end{bmatrix} \begin{bmatrix} \dot{u}_i \\ \dot{\nu}_i \\ \dot{r}_i \end{bmatrix} + \begin{bmatrix} -m_{22}\nu_i r_i - m_{23} r_i^2 \\ m_{11} u_i r_i \\ (m_{22} - m_{11}) u_i \nu_i + m_{23} u_i r_i \end{bmatrix} + \begin{bmatrix} d_{11} & 0 & 0 \\ 0 & d_{22} & d_{23} \\ 0 & d_{23} & d_{33} \end{bmatrix} \begin{bmatrix} u_i \\ \nu_i \\ r_i \end{bmatrix} = \begin{bmatrix} F_i \\ 0 \\ T_i \end{bmatrix} + \begin{bmatrix} w_{ui} \\ w_{\nu i} \\ w_{ri} \end{bmatrix}, \quad (4)$$

where, $m_{(\cdot)}$'s are the vessel's inertia parameters, $d_{(\cdot)}$'s are the hydrodynamic damping coefficients, F_i and T_i are the surge force and yaw moment, and $w_{(\cdot)}$'s denote bounded disturbances containing the model uncertainties and external disturbances. Note importantly that the dynamics (4) can represent those with general non-diagonal mass and non-diagonal damping matrices.

One can rewrite the surge system in (4) into the nonlinear system (3) with

$$f_{ui} = \frac{m_{22}\nu_i r_i + m_{23} r_i^2 - d_{11} u_i}{m_{11}}, b_{ui} = \frac{1}{m_{11}}, \delta_{ui} = \frac{w_{ui}}{m_{11}}.$$

In addition, we rewrite the sway and yaw systems as follows

$$\begin{bmatrix} \dot{\nu}_i \\ \dot{r}_i \end{bmatrix} = \begin{bmatrix} m_{22} & m_{23} \\ m_{23} & m_{33} \end{bmatrix}^{-1} \Bigg(- \begin{bmatrix} m_{11} u_i r_i \\ (m_{22} - m_{11}) u_i \nu_i + m_{23} u_i r_i \end{bmatrix} - \begin{bmatrix} d_{22} & d_{23} \\ d_{23} & d_{33} \end{bmatrix} \begin{bmatrix} \nu_i \\ r_i \end{bmatrix} \Bigg) + \begin{bmatrix} m_{22} & m_{23} \\ m_{23} & m_{33} \end{bmatrix}^{-1} \Bigg(\begin{bmatrix} w_{\nu i} \\ w_{ri} \end{bmatrix} + \begin{bmatrix} 0 \\ T_i \end{bmatrix} \Bigg)$$
$$:= \begin{bmatrix} f_{\nu i} \\ f_{ri} \end{bmatrix} + \begin{bmatrix} \delta_{\nu i} \\ \delta_{ri} \end{bmatrix} + \frac{1}{m_{22}m_{33} - m_{23}^2} \begin{bmatrix} -m_{23} T_i \\ m_{22} T_i \end{bmatrix}, \quad (5)$$

where $f_{\nu i} = f_{\nu i}(u_i, \nu_i, r_i)$, $f_{ri} = f_{ri}(u_i, \nu_i, r_i)$, and

$$\begin{bmatrix} \delta_{\nu i} \\ \delta_{ri} \end{bmatrix} := \frac{1}{m_{22}m_{33} - m_{23}^2} \begin{bmatrix} m_{33} & -m_{23} \\ -m_{23} & m_{22} \end{bmatrix} \begin{bmatrix} w_{\nu i} \\ w_{ri} \end{bmatrix}.$$

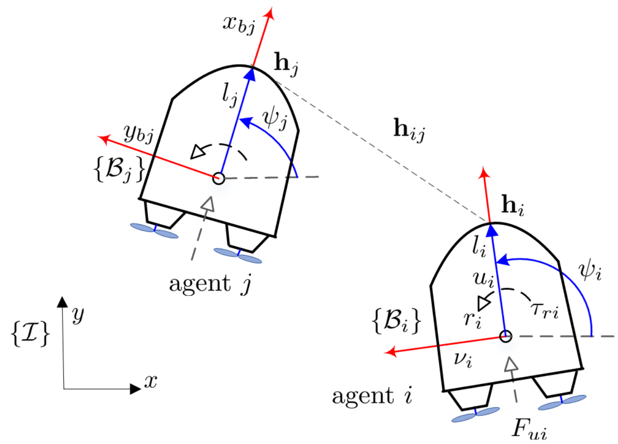

Fig. 1: Coordinate systems, the control system, and the relative position $\boldsymbol{h}_{ij} \in \mathbb{R}^2$ between two planar vehicles (e.g., underactuated surface vessels). Each agent has 3 DOFs (surge, sway, and yaw).

By (5), $b_{\nu i}$ and b_{ri} in (3) are respectively given as

$$b_{\nu i} = \frac{-m_{23}}{m_{22}m_{33} - m_{23}^2},\ b_{ri} = \frac{m_{22}}{m_{22}m_{33} - m_{23}^2}.$$

Note also that, in the above terms, we assume $m_{22}m_{33} - m_{23}^2 > 0$, considering the fact that diagonal terms m_{22}, m_{33} are usually larger than the coupling term m_{23} in practical systems.

C. Formation tracking control problem

For each agent i, we select a hand point $\boldsymbol{h}_i$ on the x_{bi}-axis with the relative vector to the central point $\boldsymbol{p}_i$ being $\boldsymbol{l}_i, ||\boldsymbol{l}_i|| = l_i$ (Fig. 1). The *displacement* vector corresponding to an edge $(i,j) \in \mathcal{E}$ is $\boldsymbol{h}_{ij} = \boldsymbol{h}_j - \boldsymbol{h}_i \in \mathbb{R}^2$. For an ordering of the edges in $\mathcal{E}$, let $\boldsymbol{H} \in \mathbb{R}^{n\times m}$ be the corresponding incidence matrix. We define $\boldsymbol{z} = \mathrm{col}(\dots, (\boldsymbol{h}_{ij})_k, \dots) \in \mathbb{R}^{2m}$ corresponding the ordering of the edges, i.e., $\boldsymbol{z}_k = \boldsymbol{h}_{ij}$ whenever the edge (i,j) is numbered as k. Then, $\boldsymbol{z} = (\boldsymbol{H}^\top \otimes \boldsymbol{I}_2)\boldsymbol{h} := \bar{\boldsymbol{H}}^\top \boldsymbol{h}$.

The leader is labeled as 1 and the set of followers is $\mathcal{V}_f = \{2, \dots, n\}$. The stacked vectors containing the followers' positions and all the agents' positions are respectively defined as

$$\boldsymbol{h}_f = \mathrm{col}(\boldsymbol{h}_2, \dots, \boldsymbol{h}_n) \in \mathbb{R}^{2n-2},$$
$$\boldsymbol{h} = \mathrm{col}(\boldsymbol{h}_1, \dots, \boldsymbol{h}_n) \in \mathbb{R}^{2n}.$$

A *formation* $(\mathcal{G}, \boldsymbol{h})$ is specified by the graph $\mathcal{G}$ and the (hand) configuration $\boldsymbol{h}$. The moving *target formation* of the system $\boldsymbol{h}^*(t) = \mathrm{col}(\boldsymbol{h}_1^*(t), \dots, \boldsymbol{h}_n^*(t)) \in \mathbb{R}^{2n}$ is characterized by the desired displacements

$$\left\{\boldsymbol{h}_{ij}^* : \boldsymbol{h}_{ij}^* = \boldsymbol{h}_j^* - \boldsymbol{h}_i^*, (i,j) \in \bar{\mathcal{E}}\right\}. \tag{6}$$

Each leader is assumed to follow the reference trajectory

$$\boldsymbol{h}_1^*(t) = \boldsymbol{h}_1^*(0) + \int_0^t \boldsymbol{v}_1^*(\tau) d\tau, \tag{7}$$

i.e., $\boldsymbol{h}_1(t) = \boldsymbol{h}_1^*(t)$, with a piece-wise constant velocity $\boldsymbol{v}_1^* \in \mathbb{R}^2$. Whereas, each follower $i \in \mathcal{V}_f$ is provided with only the desired displacements $\{\boldsymbol{h}_{ij}^*\}_{j\in\mathcal{N}_i}$ to its neighbors. The graph $\mathcal{G}$ that embeds the displacement constraints $\boldsymbol{h}_{ij}$ between the agents satisfy the following assumption.

Assumption 1: The graph $\mathcal{G}$ contains a spanning tree rooted in the leader node.

The Laplacian matrix associated with the graph $\mathcal{G}$ is $\mathcal{L}$. Define $\bar{\boldsymbol{L}} =: \mathcal{L} \otimes \boldsymbol{I}_2 \in \mathbb{R}^{2n\times 2n}$ and a partition of it as

$$\bar{\boldsymbol{L}} = \begin{bmatrix} \bar{\boldsymbol{L}}_{ll} & \bar{\boldsymbol{L}}_{lf} \\ \bar{\boldsymbol{L}}_{fl} & \bar{\boldsymbol{L}}_{ff} \end{bmatrix},$$

where $\bar{\boldsymbol{L}}_{ll} \in \mathbb{R}^{2\times 2}, \bar{\boldsymbol{L}}_{lf}, \bar{\boldsymbol{L}}_{fl}^\top \in \mathbb{R}^{2\times 2(n-1)}$ and $\bar{\boldsymbol{L}}_{ff} \in \mathbb{R}^{2(n-1)\times 2(n-1)}$. Note importantly that under Assumption 1 and the presence of the leader 1, $\bar{\boldsymbol{L}}_{ff}$ is invertible [19, Corollary 3] and has positive eigenvalues. Furthermore, one can compute the unique followers' positions in the target formation (relative to the leader's position $\boldsymbol{h}_1(t)$) as [19]

$$\boldsymbol{h}_f^*(t) = -\bar{\boldsymbol{L}}_{ff}^{-1}\bar{\boldsymbol{L}}_{fl}\boldsymbol{h}_1(t) - \bar{\boldsymbol{L}}_{ff}^{-1}\left[\bar{\boldsymbol{L}}_{fl}\ \bar{\boldsymbol{L}}_{ff}\right]\boldsymbol{h}^*(t). \tag{8}$$

That is, the desired positions of the followers $\boldsymbol{h}_f^*$ can be uniquely computed from $\boldsymbol{h}_1^*(t)$ and the desired displacements $\{\boldsymbol{h}_{ij}^*\}$, as inferred from the product $\left[\bar{\boldsymbol{L}}_{fl}\ \bar{\boldsymbol{L}}_{ff}\right]\boldsymbol{h}^*$.

Define the control error vectors $\boldsymbol{\delta}(t) := \boldsymbol{h}(t) - \boldsymbol{h}^*(t) \in \mathbb{R}^{2n}1$ and $\boldsymbol{\delta}_f(t) := \boldsymbol{h}_f(t) - \boldsymbol{h}_f^*(t) \in \mathbb{R}^{2n-2}$. Consequently, $\boldsymbol{\delta} = \mathrm{col}(\boldsymbol{0}_2, \boldsymbol{\delta}_f)$ since $\boldsymbol{h}_1(t) = \boldsymbol{h}_1^*(t)$ by assumption.

Since the sway speed is not controlled (see (4)), its boundedness might not be guaranteed. To simplify the stability analysis, the stability of the lateral motion is often assumed in works that address the coordination control of underactuated surface vessels [14]–[16].

The tracking control problem under investigation is now stated.

Problem 1: Let Assumption 1 hold, design a tracking control law at the dynamic level (F_i, T_i) for each agent $i \in \mathcal{V}_f$ so that $\boldsymbol{\delta}(t) \to \boldsymbol{0}$ asymptotically based on the inter-agent displacements $\{\boldsymbol{h}_{ij}(t)\}_{j\in\mathcal{N}_i}$.

III. Proposed Tracking Control Scheme

A tracking controller is proposed based on inter-agent displacements for a group of underactuated agents whose dynamics is described by (3). For this, the motion equation of the hand point as an *output regulation system* is derived [13]; while the vessel's *internal dynamics* is composed of the sway and yaw dynamics. Lastly, we prove the global exponential stability of the target formation.

A. The motion of the hand points

Let $\boldsymbol{v}_{hi}^i \in \mathbb{R}^2$ and $\boldsymbol{a}_{hi}^i \in \mathbb{R}^2$ be the local coordinates of the velocity and acceleration of the hand point $\boldsymbol{h}_i$, respectively. We have the following relations

$$\boldsymbol{v}_{hi}^i = \boldsymbol{R}_i^\top \dot{\boldsymbol{h}}_i \text{ and } \boldsymbol{a}_{hi}^i = \boldsymbol{R}_i^\top \ddot{\boldsymbol{h}}_i, \forall i \in \mathcal{V}.$$

Let $\vec{k}$ be the normal vector of the motion plane. Thus, the hand point's velocity and acceleration can be respectively computed using the geometric constraint $\boldsymbol{h}_i = \boldsymbol{p}_i + \boldsymbol{l}_i$ by

$$\vec{v}_{hi} = \vec{v}_i + r_i\vec{k} \times \vec{l}_i,$$
$$\vec{a}_{hi} = \dot{\vec{v}}_i + \dot{r}_i\vec{k} \times \vec{l}_i - r_i^2\vec{l}_i.$$

Expressing the preceding relations in each local coordinate system $\{\mathcal{B}_i\}$ gives

$$\boldsymbol{v}_{hi}^i = \begin{bmatrix} u_i \\ \nu_i + r_i l_i \end{bmatrix}, \tag{9}$$

$$\begin{aligned}\boldsymbol{a}_{hi}^i &= \begin{bmatrix} \dot{u}_i - r_i^2 l_i \\ \dot{\nu}_i + \dot{r}_i l_i \end{bmatrix} \\ &\overset{(3)}{=} \begin{bmatrix} f_{ui} + \delta_{ui} - r_i^2 l_i + b_{ui}F_{ui} \\ f_{\nu i} + l_i f_{ri} + \delta_{\nu i} + l_i\delta_{ri} + (b_{\nu i} + b_{ri}l_i)\tau_{ri} \end{bmatrix},\end{aligned} \tag{10}$$

which implies that $\boldsymbol{h}_i(t)$ can be regulated by designing (F_{ui}, τ_{ri}). In the following subsections, a control protocol will be proposed based on this system to drive the agents' hand points to the target formation, thus solving Problem 1. Nevertheless, as can be seen from (9), the (ν_i, r_i)-system in (3) constituting the vehicle's internal dynamics is uncontrolled. The stability of the internal dynamics of the agents under certain conditions will be investigated later.

B. Formation tracking controller with a constant velocity leader

Define a sliding surface vector $\boldsymbol{s}_i = \boldsymbol{R}_i(\psi_i)\boldsymbol{s}_i^i$ for each agent i with the local coordinates $\boldsymbol{s}_i^i = [s_{1i}, s_{2i}]^\top$ as follows

$$\begin{aligned}\boldsymbol{s}_i = \dot{\boldsymbol{h}}_i &- k_P\sum_{j\in\mathcal{N}_i}(\boldsymbol{h}_{ij} - \boldsymbol{h}_{ij}^*) \\ &- k_I\int_0^t \sum_{j\in\mathcal{N}_i}(\boldsymbol{h}_{ij}(\tau) - \boldsymbol{h}_{ij}^*)d\tau,\end{aligned} \tag{11}$$

where $k_P, k_I > 0$ are control gains. The goal is to stabilize the sliding surface vector $\boldsymbol{s}_i$ to the origin exponentially fast, on the sliding surface $\boldsymbol{s}_i = 0$, as we will show, $\boldsymbol{h}_i$ converge to the desired formation asymptotically. To proceed, we compute the derivative of the vector $\boldsymbol{s}_i^i$ (since $\boldsymbol{s}_i^i = \boldsymbol{R}_i(\psi_i)^\top\boldsymbol{s}_i$) as

$$\begin{aligned}\dot{\boldsymbol{s}}_i^i &= \dot{\boldsymbol{R}}_i^\top\boldsymbol{s}_i + \boldsymbol{R}_i^\top\dot{\boldsymbol{s}}_i = r_i\begin{bmatrix} s_{2i} \\ -s_{1i} \end{bmatrix} + \boldsymbol{R}_i^\top\dot{\boldsymbol{s}}_i \\ &\overset{(11)}{=} r_i\begin{bmatrix} s_{2i} \\ -s_{1i} \end{bmatrix} + \boldsymbol{a}_{hi}^i - \boldsymbol{R}_i^\top\sum_{j\in\mathcal{N}_i}\Big(k_P(\dot{\boldsymbol{h}}_j - \dot{\boldsymbol{h}}_i) \\ &\quad + k_I(\boldsymbol{h}_j - \boldsymbol{h}_i)\Big)\end{aligned} \tag{12}$$

The control input for each agent i can be designed as

$$\begin{aligned}\begin{bmatrix} b_{ui}F_{ui} \\ (b_{\nu i}l_i + b_{ri})\tau_{ri} \end{bmatrix} &= -k_s\boldsymbol{s}_i^i - \beta\,\mathrm{sign}(\boldsymbol{s}_i^i) - \begin{bmatrix} f_{ui} - r_i^2 l_i \\ f_{\nu i} + l_i f_{ri} \end{bmatrix} \\ &+ \boldsymbol{R}_i^\top\sum_{j\in\mathcal{N}_i}\Big(k_P(\dot{\boldsymbol{h}}_j - \dot{\boldsymbol{h}}_i) + k_I(\boldsymbol{h}_j - \boldsymbol{h}_i)\Big).\end{aligned} \tag{13}$$

Here, $k_s > 0$ and $\beta > 0$ is a sufficiently large constant such that $\beta > \|[\delta_{ui}, \delta_{\nu i} + l_i\delta_{ri}]\|_\infty$. When the upper bounds $|\delta_{ui}| \leq \Delta_{u,i}$, $|\delta_{\nu i}| \leq \Delta_{\nu,i}$ and $|\delta_{ri}| \leq \Delta_{r,i}$ are known by each agent i, one can choose $\beta > \max\{\Delta_{u,i}, \Delta_{\nu,i} + l_i\Delta_{r,i}\}$. The displacements and relative velocities between neighboring agents are required to compute the control law (13).

C. Stability analysis

Exponential convergence to the origin of the sliding surface variable $\boldsymbol{s}_i$ is proved for each agent as follows.

Lemma 1: Under Assumption 1 and the control law (13) with $\beta > \|[\delta_{ui}, \delta_{\nu i} + l_i\delta_{ri}]\|_\infty$, $\boldsymbol{s}_i \to 0$ exponentially as time diverges.

Proof: The time derivative of the Lyapunov function $V = \frac{1}{2}||\boldsymbol{s}_i||^2 = \frac{1}{2}||\boldsymbol{s}_i^i||^2$ under the evolution of (12) with respect to time can be proved to be negative definite

$$\begin{aligned}\dot{V}(t) &= (\boldsymbol{s}_i^i)^\top\dot{\boldsymbol{s}}_i^i \\ &= -k\|\boldsymbol{s}_i^i\|^2 - \beta(\boldsymbol{s}_i^i)^\top\mathrm{sign}(\boldsymbol{s}_i^i) + (\boldsymbol{s}_i^i)^\top\begin{bmatrix} \delta_{ui} \\ \delta_{\nu i} + l_i\delta_{ri} \end{bmatrix} \\ &\leq -k\|\boldsymbol{s}_i^i\|^2 \leq -k\|\boldsymbol{s}_i\|^2.\end{aligned} \tag{14}$$

It follows that $\boldsymbol{s}_i \to \boldsymbol{0}$ exponentially fast as $t \to \infty$. ■

Let

$$\boldsymbol{\xi}_i = -\int_0^t \sum_{j\in\mathcal{N}_i}(\boldsymbol{h}_{ij}(\tau) - \boldsymbol{h}_{ij}^*),$$
$$\boldsymbol{s} = \mathrm{col}(\boldsymbol{s}_2, \ldots, \boldsymbol{s}_n),\ \boldsymbol{\xi}_f = \mathrm{col}(\boldsymbol{\xi}_2, \ldots, \boldsymbol{\xi}_n) \in \mathbb{R}^{2(n-1)}.$$

We can now obtain the following theorem.

Theorem 1: Let Assumption 1 hold. Under the action of controller (13) with $\beta > \|[\delta_{ui}, \delta_{\nu i} + l_i\delta_{ri}]\|_\infty$, the system achieves the target formation asymptotically and exponentially fast as time diverges.

Proof: By (11), one gets the following system

$$\begin{aligned}\dot{\boldsymbol{h}}_f &= -k_P\big[\bar{\boldsymbol{L}}_{fl}\ \bar{\boldsymbol{L}}_{ff}\big](\boldsymbol{h} - \boldsymbol{h}^*) - k_I\boldsymbol{\xi}_f + \boldsymbol{s}(t) \\ &= -k_P\Big(\bar{\boldsymbol{L}}_{fl}\boldsymbol{h}_1 - \bar{\boldsymbol{L}}_{ff}\boldsymbol{h}_f - \big[\bar{\boldsymbol{L}}_{fl}\ \bar{\boldsymbol{L}}_{ff}\big]\boldsymbol{h}^*\Big) \\ &\quad + k_I\boldsymbol{\xi}_f + \boldsymbol{s}(t),\end{aligned} \tag{15}$$

$$\dot{\boldsymbol{\xi}}_f = \big[\bar{\boldsymbol{L}}_{fl}\ \bar{\boldsymbol{L}}_{ff}\big](\boldsymbol{h} - \boldsymbol{h}^*). \tag{16}$$

By (8), the formation error is given as

$$\begin{aligned}\boldsymbol{\delta}_f &:= \boldsymbol{h}_f - \boldsymbol{h}_f^* \\ &\overset{(8)}{=} \boldsymbol{h}_f + \bar{\boldsymbol{L}}_{ff}^{-1}\bar{\boldsymbol{L}}_{fl}\boldsymbol{h}_1 + \bar{\boldsymbol{L}}_{ff}^{-1}[\bar{\boldsymbol{L}}_{fl}\ \bar{\boldsymbol{L}}_{ff}]\boldsymbol{h}^*,\end{aligned}$$

and hence $\dot{\boldsymbol{\delta}}_f = \dot{\boldsymbol{h}}_f + \bar{\boldsymbol{L}}_{ff}^{-1}\bar{\boldsymbol{L}}_{fl}\dot{\boldsymbol{h}}_1 := \dot{\boldsymbol{h}}_f - \dot{\boldsymbol{h}}_f^*$, where $\dot{\boldsymbol{h}}_f^*$ denotes the desired velocity of the followers. As a result, we express the preceding system as a linear system with an input

$$\begin{aligned}\begin{bmatrix} \dot{\boldsymbol{\delta}}_f \\ \dot{\boldsymbol{\xi}}_f \end{bmatrix} &= \begin{bmatrix} -k_P\bar{\boldsymbol{L}}_{ff} & -k_I\boldsymbol{I}_{n-1} \\ \bar{\boldsymbol{L}}_{ff} & \boldsymbol{0} \end{bmatrix}\begin{bmatrix} \boldsymbol{\delta}_f \\ \boldsymbol{\xi}_f \end{bmatrix} \\ &\quad + \begin{bmatrix} \bar{\boldsymbol{L}}_{ff}^{-1}\bar{\boldsymbol{L}}_{fl}\dot{\boldsymbol{h}}_1 + \boldsymbol{s}(t) \\ \boldsymbol{0} \end{bmatrix}.\end{aligned} \tag{17}$$

One can show that the state matrix in (17) is Hurwitz and hence $(\boldsymbol{\delta}_f, \boldsymbol{\xi}_f)$ in (17) is uniformly ultimately bounded. This together with the fact that $\boldsymbol{s}(t)$ vanishes exponentially as time diverges imply the exponential convergence of the equilibrium of the system (17). Setting $\dot{\boldsymbol{\delta}}_f = \boldsymbol{0}$, $\dot{\boldsymbol{\xi}}_f = \boldsymbol{0}$ and $\boldsymbol{s} = \boldsymbol{0}$ yield the steady-state vectors $\boldsymbol{\delta}_f(\infty) = \boldsymbol{0}$ and

$\boldsymbol{\xi}_f(\infty) = \bar{\boldsymbol{L}}_{ff}^{-1}\bar{\boldsymbol{L}}_{fl}\dot{\boldsymbol{h}}_1/k_I$. Asymptotic stability and exponential convergence to the target formation of the followers follow from $\dot{\boldsymbol{\delta}}_f \to \mathbf{0}$ and $\boldsymbol{\delta}_f \to \mathbf{0}$ as $t \to \infty$. ■

Remark 1: When the velocity of the leader is time-varying, the following sliding surface vector can be designed

$$\boldsymbol{s}_i = \dot{\boldsymbol{h}}_i - |\mathcal{N}_i|^{-1}\sum_{j\in\mathcal{N}_i}(\boldsymbol{h}_{ij} - \boldsymbol{h}_{ij}^* + \dot{\boldsymbol{h}}_j), \quad (18)$$

where $\dot{\boldsymbol{h}}_j$'s are velocity feedback from neighbors. On the sliding surface $\boldsymbol{s} = 0$, one has

$$\sum_{j\in\mathcal{N}_i}(\dot{\boldsymbol{h}}_j - \dot{\boldsymbol{h}}_i) + \sum_{j\in\mathcal{N}_i}(\boldsymbol{h}_j - \boldsymbol{h}_i - \boldsymbol{h}_{ij}^*) = 0,$$

which implies that $\sum_{j\in\mathcal{N}_i}(\boldsymbol{h}_{ij} - \boldsymbol{h}_{ij}^*) \to \mathbf{0}$ asymptotically and exponentially fast as $t \to \infty$ for $i = 2, \ldots, n$. Thus, $[\bar{\boldsymbol{L}}_{fl}\ \bar{\boldsymbol{L}}_{ff}](\boldsymbol{h} - \boldsymbol{h}^*) = \bar{\boldsymbol{L}}_{ff}\boldsymbol{\delta}_f \to 0$ as $t \to \infty$, that is, the system achieves the target formation asymptotically. The derivative of the sliding surface vector is given as

$$\dot{\boldsymbol{s}}_i^i = r_i\begin{bmatrix} s_{2i} \\ -s_{1i}\end{bmatrix} + \boldsymbol{a}_{hi}^i - |\mathcal{N}_i|^{-1}\boldsymbol{R}_i^\top\sum_{j\in\mathcal{N}_i}(\dot{\boldsymbol{h}}_j - \dot{\boldsymbol{h}}_i + \ddot{\boldsymbol{h}}_j).$$

Thus, the control input for vessel i can be proposed as in (13) with the last term in (13) replaced with $|\mathcal{N}_i|^{-1}\boldsymbol{R}_i^\top\sum_{j\in\mathcal{N}_i}(\dot{\boldsymbol{h}}_j - \dot{\boldsymbol{h}}_i + \ddot{\boldsymbol{h}}_j)$. However, this controller requires the acceleration feedback, it is hard to measure it precisely in practice.

D. Sufficient condition for stable internal dynamics

This subsection provides a sufficient condition on the leader's velocity and hand points' positions for stable internal dynamics. From the relation $\boldsymbol{v}_{hi}^i = \boldsymbol{R}_i^\top\dot{\boldsymbol{h}}_i = [u_i, \nu_i + r_il_i]^\top$ (see (9)) and the exponential convergence of $\dot{\boldsymbol{h}}_i$ to $\dot{\boldsymbol{h}}_i^*$ (Theorem 1), u_i and $\nu_i + r_il_i$ are ultimately bounded. It thus suffices to show the uniform ultimate boundedness (UUB) of ν_i, implying the UUB of the yaw rate r_i.

The sway dynamics is given as the second row of (4), i.e.,

$$\dot{\nu}_i = \frac{1}{m_{22}}(-m_{23}\dot{r}_i - m_{11}u_ir_i - d_{22}\nu_i - d_{23}r_i + w_{\nu i}). \quad (19)$$

Let the local and global coordinates of the hand point's velocity be $\boldsymbol{v}_{hi}^i := [u_{h_i}, \nu_{h_i}]^\top$ and $\dot{\boldsymbol{h}}_i = [\dot{h}_{ix}, \dot{h}_{iy}]^\top$, respectively. As a result, u_{h_i}, ν_{h_i} are bounded due to $||\boldsymbol{v}_{hi}^i|| = ||\boldsymbol{R}_i^\top\dot{\boldsymbol{h}}_i|| = ||\dot{\boldsymbol{h}}_i||$. By (9), the sway velocity and yaw rate respectively are

$$u_i = u_{h_i},\ r_i = \frac{1}{l_i}(\nu_{h_i} - \nu_i). \quad (20)$$

Substituting the preceding relations into (19) yields the internal dynamics of the vessels

$$\begin{aligned}\dot{\nu}_i &= \frac{1}{m_{22}}\big[-m_{23}\dot{r}_i - m_{11}l_i^{-1}u_{hi}(\nu_{hi} - \nu_i) - d_{22}\nu_i \\ &\quad - d_{23}l_i^{-1}(\nu_{hi} - \nu_i) + w_{\nu i}\big] \\ &= -\frac{m_{23}}{m_{22}}\dot{r}_i - \frac{1}{m_{22}}(d_{22} - m_{11}l_i^{-1}u_{hi} - d_{23}l_i^{-1})\nu_i \\ &\quad + \frac{1}{m_{22}}(-m_{11}l_i^{-1}u_{hi}\nu_{hi} - d_{23}l_i^{-1}\nu_{hi} + w_{\nu i}). \quad (21)\end{aligned}$$

Theorem 2: Suppose that Assumption 1 holds and consider the internal dynamics (19). If the target velocity of vessel i satisfies $||\dot{\boldsymbol{h}}_i^*(t)|| < \frac{d_{22}l_i - d_{23}}{m_{11}}$ and the hand point's offset $l_i > \max\{d_{23}/d_{22}, m_{23}/m_{22}\}$ then under the action of the controller (13), the internal dynamics of the system is uniformly ultimately bounded (UUB).

The proof of Theorem 2 can be shown by following similar lines as Proofs of Lemma 1 and Theorem 3 in [13] and thus omitted to save space.

Theorem 2 implies that to guarantee the boundedness of the internal dynamics (21) one should select the desired formation velocity sufficiently small and the hand points' locations are large enough.

IV. Simulation

Simulation results of the formation tracking control of six underactuated surface vehicles with a constant velocity leader under the controller (13) are provided in Fig. 2. The target formation $(\bar{\mathcal{G}}, \boldsymbol{h}^*)$ of the multi-vessel system is depicted in Fig. 2a, which is formed by two squares of length 10 meters. It is checked that the graph contains a spanning tree rooted at the leader node 1 (Fig. 2a). For the simulation, the dynamical models of the agents are chosen differently. The dynamical parameters for vessels 5 and 6 with diagonal mass and hydrodynamic damping matrices are given as $m_{11} = 200$ kg, $m_{22} = 250$ kg, $m_{23} = 0$ kg, $m_{33} = 700$ kg.m^2, $d_{11} = 70$ kg/s, $d_{22} = 100$ kg/s, $d_{33} = 50$ kg.m^2/s, $d_{23} = 0$ kgm/s, and $l_i = 1.6$ (m). The model parameters of vessels from 1 to 4 are $m_{11} = 200$ kg, $m_{22} = 300$ kg, $m_{33} = 750$ kg.m^2, $m_{23} = 3$ kgm, $d_{11} = 70$ kg/s, $d_{22} = 100$ kg/s, $d_{33} = 50$ kg.m^2/s, $d_{23} = -30$ kgm/s, and $l_i = 1.4$ m. The disturbance components acted upon (3) are given as $\delta_{ui} = 0.5 + 0.15\sin(2t) + 0.15\sin(10t)$, $\delta_{\nu i} = 0$, and $\delta_{ri} = (3/7) + (6/7)\sin(2t) + (4/7)\sin(10t)$.

In the simulation, the leader agent 1 moves with the constant surge speed $u_1 = 0.5$ m/s and constant yaw angle $\psi_1 = \pi/6$ rad. The control gains are selected as $k_s = 5, \beta = 2, k_P = 2$ and $k_I = 1$. One verifies that $||\dot{\boldsymbol{h}}_i^*|| = 0.5 < \frac{d_{22}l_i - d_{23}}{m_{11}} = 0.85$ m/s for vessels from 1 to 4 (< 0.8 for vessels 5 and 6) and $l_i > \max\{d_{23}/d_{22}, m_{23}/m_{22}\} = 0.012$ m for all vessels, satisfying the conditions in Theorem 2. As observed from Fig. 2d, the vessel system arrives at the target formation asymptotically since the control errors $\boldsymbol{\delta}_f \to 0$ and $\dot{\boldsymbol{\delta}}_f \to 0$ as $t \to \infty$ (Fig. 2c). The yaw angles of the vessels tend to converge to that of the leader vessel asymptotically, as depicted in Fig. 2b.

V. Conclusion

In this work, a robust formation tracking control scheme was proposed for a group of heterogeneous underactuated agents based on the inter-agent displacements. Due to the underactuation of the agents, the presented control protocol aims to regulate certain points on the longitudinal axis, different from the central points, to track the moving formation. Specifically, under the action of the proposed tracking controller, the hand points of the agents are steered to the

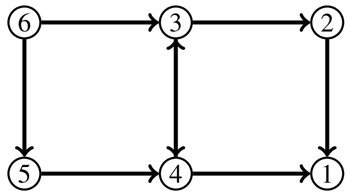

(a) The interaction graph $\mathcal{G}$ and the desired formation (two squares of side length 10 m) of the system.

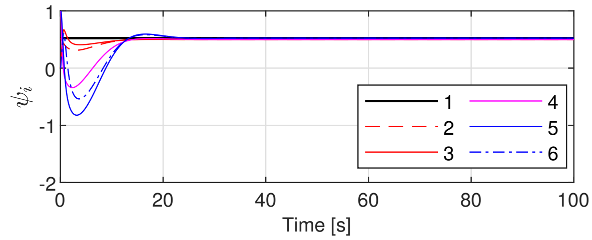

(b) Yaw angles [rad] vs time.

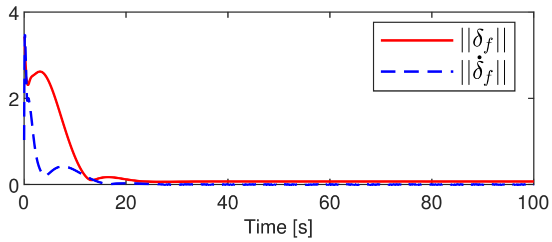

(c) Tracking control errors vs time.

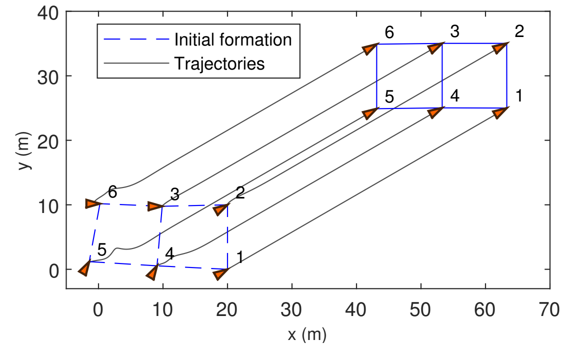

(d) Trajectories of the agents under the control law (13).

Fig. 2: Six heterogeneous surface vessels track a moving formation.

target formation asymptotically and with an exponential convergence rate. We subsequently showed that to guarantee the boundedness of the internal dynamics, the desired formation velocity is required to be sufficiently small and the hand points' locations large enough. A potential extension of the proposed control approach is investigating model-free robust formation tracking control schemes for underactuated planar agents.

REFERENCES

[1] H.-S. Ahn, *Formation Control: Approaches for Distributed Agents*. Springer International Publishing, 2019.

[2] Q. V. Tran, H.-S. Ahn, and J. Kim, "Direction-only orientation alignment of leader-follower networks," in *in Proc. the 2022 American Control Conference (ACC)*, 2022, pp. 2142–2147.

[3] Q. V. Tran, M. H. Trinh, N. H. Nguyen, and H.-S. Ahn, "Free-will arbitrary time consensus protocols with diffusive coupling," *International Journal of Robust and Nonlinear Control*, vol. 32, no. 15, pp. 8711–8731, 2022.

[4] X. Du, W. Li, J. Xiao, and Z. Chen, "Time-varying group formation with leader-following control for heterogeneous multi-agent systems," *Int. J. Control Autom. Syst.*, vol. 21(7), pp. 2087–2098, 2023.

[5] Q. V. Tran, "Fixed-time localization of local coordinate frames: Interpretation and applications to formation control problems," *Int. J. Control Autom. Syst.*, pp. 1–8, 2023, minor revision.

[6] T. I. Fossen, *Marine Control Systems*. Trondheim, Norway: Marine Cybernetics, 2002.

[7] S. Han, M. Choi, M. Cho, J. il Park, and K.-S. Kim, "Dynamic control and simulation of leader-follower vehicle formation considering vehicle stability," *Int. J. Control Autom. Syst.*, vol. 21(9), pp. 2995–3005, 2023.

[8] Q. V. Tran and J. Kim, "Bearing-constrained formation tracking control of nonholonomic agents without inter-agent communication," *IEEE Control Syst. Lett.*, vol. 6, pp. 2401–2406, Mar. 2022.

[9] F. Fahimi, "Sliding-mode formation control for underactuated surface vessels," *IEEE Trans. Rob.*, vol. 23, no. 3, pp. 617–622, Jun. 2007.

[10] Z. Peng, J. Wang, D. Wang, and Q.-L. Han, "An overview of recent advances in coordinated control of multiple autonomous surface vehicles," *IEEE Trans. Ind. Inf.*, vol. 17, no. 2, pp. 732–745, 2021.

[11] X. Li, C. Wen, X. Fang, and J. Wang, "Adaptive bearing-only formation tracking control for nonholonomic multiagent systems," *IEEE Trans. Cybern.*, vol. 52, no. 8, pp. 7552–7562, 2022.

[12] C. Lee, Q. V. Tran, and J. Kim, "Robust path tracking and obstacle avoidance using tube-based model predictive control for surface vehicles," *IFAC-PapersOnLine*, vol. 55, no. 31, pp. 301–306, 2022, 14th IFAC Conference on Control Applications in Marine Systems, Robotics, and Vehicles CAMS 2022.

[13] Q. V. Tran, C. Lee, J. Kim, and H. Q. Nguyen, "Robust bearing-based formation tracking control of underactuated surface vessels: An output regulation approach," *IEEE Transactions on Control of Network Systems*, no. 1, pp. 1–12, 2023.

[14] X. Jin, "Fault tolerant finite-time leader-follower formation control for autonomous surface vessels with LOS range and angle constraints," *Automatica*, vol. 68, pp. 228–236, 2016.

[15] Y. Lu, G. Zhang, L. Qiao, and W. Zhang, "Adaptive output-feedback formation control for underactuated surface vessels," *International Journal of Control*, vol. 93, no. 3, pp. 400–409, 2020.

[16] B. Wang, S. Nersesov, and H. Ashrafiuon, "Robust formation control and obstacle avoidance for heterogeneous underactuated surface vessel networks," *IEEE Trans. Control Network. Syst.*, vol. 9, no. 1, pp. 125–137, 2022.

[17] Y. Zhang, S. Wang, X. Wang, and X. Tian, "Bearing-based formation control for multiple underactuated autonomous surface vehicles with flexible size scaling," *Ocean Engineering*, vol. 267, p. 113242, Jan. 2023.

[18] F. Bullo, *Lectures on Network Systems*, 1st ed. Kindle Direct Publishing, 2020, with contributions by J. Cortes, F. Dorfler, and S. Martinez. [Online]. Available: http://motion.me.ucsb.edu/book-lns

[19] Q. V. Tran and H.-S. Ahn, "Distributed formation control of mobile agents via global orientation estimation," *IEEE Trans. Control Network Syst.*, vol. 4, no. 7, pp. 1654–1664, 2020.